



HAL
open science

In-depth influence of the top surface fabrication of a bead packing

Luc Oger, Renaud Delannay, Yves Le Gonidec

► **To cite this version:**

Luc Oger, Renaud Delannay, Yves Le Gonidec. In-depth influence of the top surface fabrication of a bead packing. *Physical Review E*, In press. hal-03886192v2

HAL Id: hal-03886192

<https://hal.science/hal-03886192v2>

Submitted on 15 Dec 2022 (v2), last revised 24 May 2023 (v3)

HAL is a multi-disciplinary open access archive for the deposit and dissemination of scientific research documents, whether they are published or not. The documents may come from teaching and research institutions in France or abroad, or from public or private research centers.

L'archive ouverte pluridisciplinaire **HAL**, est destinée au dépôt et à la diffusion de documents scientifiques de niveau recherche, publiés ou non, émanant des établissements d'enseignement et de recherche français ou étrangers, des laboratoires publics ou privés.

Copyright

In-depth influence of the top surface fabrication of a bead packing

Luc Oger  and Renaud Delannay 

*Univ. Rennes, CNRS, IPR [(Institut de Physique de Rennes)]-UMR 6251, F-35000 Rennes, France**

Yves Le Gonidec 

Univ. Rennes, CNRS, Géosciences Rennes-UMR 6118, F-35000 Rennes, France

(Dated: December 2, 2022)

Packings of beads confined in slowly tilted containers with a top open surface are commonly used in laboratory experiments to model natural grain avalanches and better understand and predict critical events from optical measurements of the surface activity. To that aim, after reproducible packing preparations (pouring then grid pulling out), the present work focuses on the effect of the surface fabrication, which can be scraped or soft leveled, on both the avalanche stability angle and the dynamic of precursory events (small surface reorganization) for glass beads of 2 mm diameter. A depth effect of a scraping operation is highlighted by considering different packing heights, up to 185 mm, and inclination speeds in the range 1.7-14°/min.

PACS numbers: 45.70.Ht, 81.05.Rm, 81.20.Ev

Keywords: granular media, precursors of avalanche, image analysis, packing preparation

I. INTRODUCTION

Understanding the mechanics of granular flows is of first importance for numerous industrial and natural domains where avalanches constitute critical events of grain displacements. It remains difficult to prevent from such instabilities because the triggering is controlled by a large number of physical parameters, including the grain shape and material, the grain pile compacity and history and the ambient humidity and temperature. Aiming at identifying the contribution of each parameter, small-scale laboratory experiments are commonly performed in controlled conditions where the granular pile consists in grains confined in a box and slowly tilted until the granular flow at the top surface starts. At rest, a granular packing can sustain normal loads and shear stresses, such as a jammed structure [1]. When the packing is tilted, the shear stress may exceed a threshold and part of the pile starts to flow and the macroscopic behavior of the packing is related to geometry changes of the contact network and more specifically to the nature of the contacts which can be frictional, collisional, sliding, or cohesive [2]. Precursory events are observed during quasi-static behavior of the inclination process, *i.e.* when bead displacement occurs only when local shear forces reach a critical value defined by the Coulomb's friction law. This behavior can be also influenced by the inclination speed of the grain container. For soft leveled surface flows, the critical shear stress is evidenced by the existence of the angle of maximum stability θ_A associated to internal friction properties [3]. When the tilt stops, the angle of the pile relaxes towards the angle of repose ($\theta_R < \theta_A$). Among the different techniques that can be used to

observe the avalanche events of a granular pile, we can point out: measuring the weight at the outlet of the packing container [4], following the surface evolution by sequential optical [5–7] or acoustical [6, 8, 9] methods.

More recently, Kiesgen de Richter et al. [10, 11] and Duranteau et al. [9, 12] have confirmed these observations by using two successive improved automatic tilting setups to study particular physical parameters that control the dynamic of grain avalanches. Indeed, the size of the system (height [4], length [6] width [13–16]), the density or volume compaction of the packing [4, 6, 17–19] and the tilting regime [12, 20, 21] are some parameters that have been studied in previous works. For example, Aguirre et al. [18] put in evidence the influence of the packing height on the maximum stability angle when the number of grain layers is lower than ten. This is particularly important when it consists in layer by layer depositions completed by series of taps of the surface in between [5]. Indeed, this can be related to the well-known 'wall effect' [22–26] obtained on few layers of grains that become quasi-ordered close to the walls of the container which have locally modified the packing fraction.

As mentioned previously, since many years, we have developed numerous experiments at the laboratory of the IPR (Institut de Physique de Rennes) to analyze precursory events of granular avalanches [9, 10, 12, 27]. These previous series of experiments were the opportunity to identify ambient (proximity of a ventilation system, humidity and temperature, etc.), experimental (dimensions and inclination speed of the grain container, parameters and synchronization of the data acquisition, etc.) and packing (electrostatic effects, compaction, fabrication, etc.) conditions that influence the reproducibility of the results. In particular, the fabrication of the granular packing and its top surface, which is often considered in the literature as part of the 'history' preparation of the grain packing, requires a particular attention for a better

* luc.oger@univ-rennes1.fr

interpretation of the results. Firstly, the present work focuses on the effects of the granular top surface fabrication on the dynamic of the packing destabilization. The parameters of the experimental setup, the fabrication of the grain packing of glass beads of 2 mm diameter, with a top surface which can be let soft leveled or metal-scraped, and the optical experiments performed to detect the precursory events are described in Section II. Section III deals with the influence of the packing height on the grain destabilization for a fixed inclination speed. In Section IV, the influence of the inclination speed is studied for both few soft leveled or scraped top granular surfaces.

II. DESCRIPTION OF THE EXPERIMENTS

A. Experimental setup in controlled conditions

The grain packing is composed of glass beads pulled in a rigid container. As, by nature, critical events of the bead avalanches are very sensitive to all the ambient conditions of the laboratory, few experimental precautions were adopted. External mechanical vibrations exist in the laboratory so the whole experimental setup is thus mounted on an optical table (Melles Griot™) managed by four pneumatic attenuators and additional damping pads (Sunnex™ SP 700, 8 mm thickness) to isolate, as much as possible, the setup from the room floor submitted to low frequencies perturbations. To avoid the influence of the ambient humidity on the bead destabilization [28], the experiments are performed in an air-conditioned room where both the temperature (between 20-23°C) and humidity (45-55% HR) are controlled.

The bead container is a parallelepipedic metallic box (adjustable length up to $L = 1000$ mm, width $W = 200$ mm and height $H = 200$ mm) and to relax electrostatic effects inside the bead packing, with a wire connection to the building ground. For our series of experiments, the length $L = 420$ and 640 mm were chosen and the available packing height H was selected between 30 and 185 mm. It is rigidly connected to a reclining plate which rotates about two horizontal ball bearing axis positioned at the center of the length L to avoid possible inhomogeneous oscillations that may be due to weight momentum. The rotation is managed by the use of a linear actuator (SKF™): the maximum force of the working piston is 7 kN and the stroke length is 700 mm. The speed is controlled, *via* an Arduino™ card, by a main LabVIEW™ program written to control the whole experiment: the speed V_i ranges between 1.7 and $14^\circ/\text{min}$. The tilt angle is measured by the use of a Sensel™ sensor and recorded by the same program through an analogical/digital acquisition USB card: in our case, the angle θ ranges between the horizontal position and a maximum angle of $\pm 30^\circ$ higher than the classical angle of maximal stability angle θ_A for simple sphere packings. The angle value is saved with the number of the image captured at

the same time through a text file as described later on.

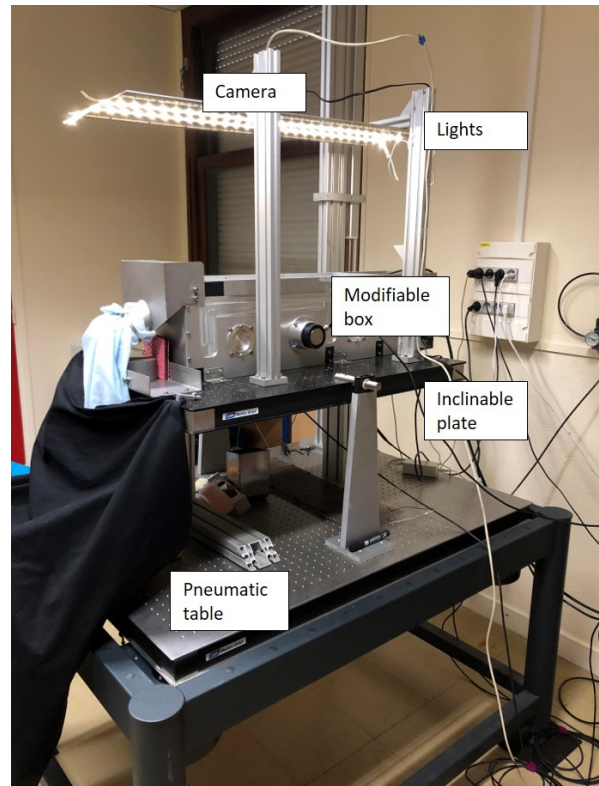


FIG. 1. Experimental setup which presents the pneumatic table, the inclinable plate, the metallic box and the optical system (camera + lights) on top which moves strongly coupled with the plate.

B. Fabrication of the bead packing

In addition to controlled environment conditions, reproducible experiments of bead destabilization also require a controlled protocol of the fabrication of the bead packing, and in particular its granular top surface. Indeed, in the present work, we achieved the so-called 'same history' of a bead packing fabrication [29] aiming at performing reproducible experiments. The bead packing consists in monodisperse glass beads of diameter $D=2$ mm (SiLiBeads type M™) randomly poured into the rigid bead container. The packing height $h \leq H$ is related to the number n_l of bead layers in the container: if n_l is small, the dynamic of the bead destabilization may depend on n_l due to the relation (distance) with the bottom wall effect [22–26].

During the preparation, a grid with a square mesh of 12 mm $\gg D$ is placed above the bottom of the bead container, then covered by the beads and then pulled out to homogenize the contact network between the beads in the whole packing volume. Then, the open top surface of the bead packing, *i.e.* the freely obtained surface, is

finally flattened by horizontally pushing different apparatus (brush or bar) to remove surface irregularities larger than a bead diameter and form an average bead packing of height h .

In the present work, series of experiments have been performed by the use of two different apparatus: a rigid metallic bar, commonly used in previous experiments [6, 9, 11], and a soft brush. Both apparatus have a width close to the inner box width. The first choice may compact and organize the superficial bead structure and result in a 'scraped surface', and the second one only minimizes these effects to maintain a 'soft leveled surface'. The aim is highlighting the impact of these methods on the dynamic of the bead destabilization.

According to this fabrication protocol, we have prepared series of bead packings with scraped or soft leveled surfaces and different heights h ranging between 30 mm ($n_l=15$) and $H_{max} = 185$ mm by inserting series of 5 mm thickness polyethylene foam plates at the bottom of the container. This solution allows us to repeatably displace the surface flattening apparatus along the two lateral walls of the metallic container and generate exactly the same top open behaviors.

C. Optical monitoring of the bead packing destabilization

To monitor the avalanche and precursory events of the bead packing during the inclination, an optical camera (Allied Vision™ Prosilica GC-2450) records images of the central part of the granular surface as a function of the tilt angle θ . The images, with a resolution of $S_0 = 2448 \times 2050$ pixels on 8 bits gray level, are recorded with a rate of 1 image/s and a high aperture of 1/15000 s to ensure clarity of bead positions. This requires a proper lighting of the packing surface, provided by four LEDs stripes glued on both side of the camera support on a rigid metallic plate parallel to the beads packing surface which turns coupled with the packing oscillation (see Fig. 1). The camera is fixed 1 m above the granular surface and the size of an image is the surface reference $S_0 = 230$ mm (length) \times 200 mm (width). Note that a 2 mm diameter bead is visible by about 25 pixels.

To detect and identify surface instabilities, we process the images according to previous approaches [6, 9, 28, 30]: it is based on an Imagej [31] script which consists in pixel differences of two consecutive images and an amplitude threshold to reduce the noise and quantify the amount of modified pixels S used to define the surface activity S/S_0 as a function of the angle θ . Note that we assume that a modified isolated small group of pixels is, by definition, linked to, at least, one bead surface displacement. Based on this ratio, the constant bead flow of the avalanche during few seconds is associated to a nearly constant activity $S/S_0 \simeq 1$ measured for $\theta > \theta_A$, with θ_A the avalanche angle (*maximum stability angle*). At lower tilt angles, the

measure of the first precursor angle θ_p (*first appearance angle*) is not obvious and can be assessed as, at a first approximation, by the first angle associated to $S/S_0 > 0.5$. Another approach is to collect the series of first precursors down to a value defining θ_p when S/S_0 connecting slope is still visible. From θ_p and θ_A , at each individual experiment, N_p precursory events can be identified, characterized by peaks of activity located at quasi-regular tilt angles $\Delta\theta$ (*inter-precursor angle*), according to:

$$\theta_A \approx \theta_p + N_p \cdot \Delta\theta, \quad (1)$$

by assuming that $\Delta\theta$ is the mean value of the inter-precursor angles measured during each experiment. In the following, these parameters are used to quantify the dynamic of the bead packing activity during gravity destabilization.

III. DYNAMIC OF A SOFT LEVELED OR SCRAPED BEAD PACKING

By performing series of experiments for different heights h of the bead packing and a fixed inclination speed of $3.3^\circ/min$, we study the influence of the method for leveling the top granular surface with a soft or rigid tool.

A. Behavior of the maximum stability angle

Series of bead packings have been prepared in a container according to the method described in Section II B. An experiment consists in slowly titling the bead container up to the avalanche which occurs at the maximum stability angle θ_A (Fig. 2). A set of a minimal number of 10 up to 20 identical experiments have been performed in order to obtain a good mean value for a set of given conditions. Indeed, note that experiments performed in the same conditions have classically 10 – 15 % of natural fluctuations induced by different bead organizations of the packing. This is the main reason of the production of a large number of successive 'identical' independent experiments to obtain a correct mean value for our measurements [32].

Soft leveling surface experiments are characterized by a continuous increase of the maximum stability angle θ_A with the packing height h (Fig. 2, disks). By construction, the full packing structure is only controlled by the first vertical extraction of the bottom grid which creates a dilute homogeneous packing. So, this evolution is only linked to the classical effect of the weight pressure of successive layers behind the surface i.e. classically defined as ρgh with ρ the packing density and h the distance between the bottom wall and the top surface which defines also the decreasing influence of the classical bottom 'wall effect' mentioned previously. Interestingly, the non linear regression curve can be also interpreted as the increase of the probability of the grains inside the packing

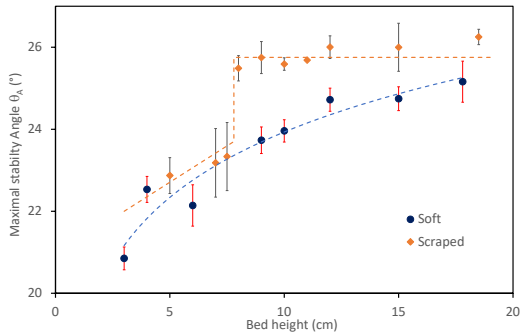


FIG. 2. Maximum stability angle θ_A measured as a function of the packing height for soft (disks) or scraped (diamonds) leveling top surfaces. Error bars are associated to at least 10 similar experiments.

to present more local contact slips linked to more complex force chains [33].

For scraped surface experiments, the angle θ_A follows a similar increase with the packing height only when $h < 7.8$ cm: the influence of the densification method by compressing several layers of superficial beads during the rolling-scraping action on the avalanche angle is weak as the number of bead layers n_l is too small to maintain this higher internal stress constraint by non-slipping contacts which allows sustainable force chains. Above this critical height, the densification method by compressing several layers of superficial beads during the rolling-scraping action can maintain this higher packing fraction inside the volume close to the surface of the packing and allows the generation of long force chains though the top volume of the packing. So, we can observe and highlight that, and when $n_l > 40$, θ_A does not depend on the packing height and the value of θ_A is almost constant around 24.5 to about 25.5°. We can note that, at the end, close to very large heights available (value of 18.5 cm in the present work), the maximum stability angles θ_A tend to be similar for both the soft leveled and the scraped surface experiments.

These results clearly highlight the effects of both the granular surface fabrication (soft or scraped) and the packing height h on the maximum stability angle θ_A of the bead packing. This more compact upper volume can handle higher maximal stability angle if the packing force chains are crossing the full sample down to the bottom wall of the packing. This densification effect can be compared with the results from [4, 18, 34]. In their experiments, the series of spoon taps on top of successive layer depositions have produced also stronger and globally denser packings and conduct at the appearance of their number of layers threshold close to 16. Indeed, compared to ours experiments in which the grid passed through them produces 'random loose' packings in both cases, only the scraped case can also create an higher

packing fraction at the upper volume.

B. Behavior of the precursory events

Before the avalanche occurs at the maximum stability angle θ_A discussed above, N_p precursory events can be detected during each experiment (Fig. 3a): the first event occurs at the angle θ_p (Fig. 3b) and the angle step between successive events is $\Delta\theta$ (Fig. 3c).

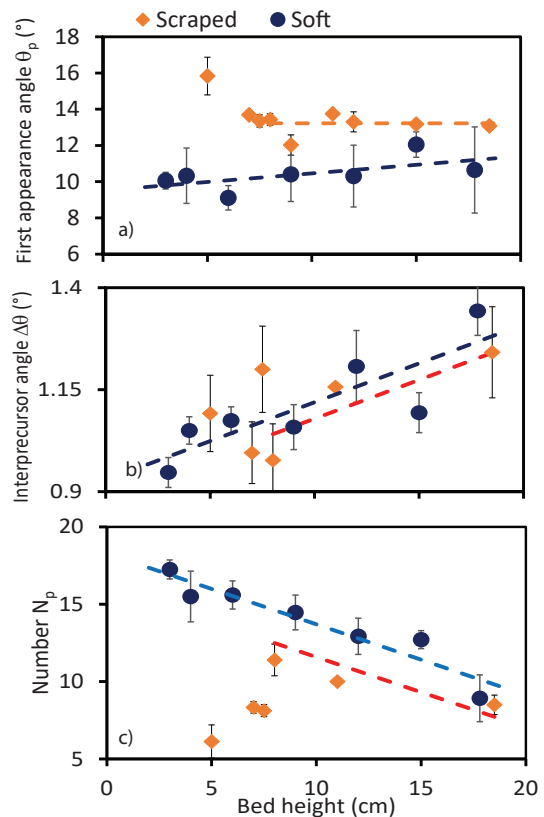


FIG. 3. Characteristic parameters of the precursory events measured as a function of the packing height with soft leveled (disks) or scraped (diamonds) surfaces.

For soft leveled surface experiments, the first appearance angles range between 9.6 and 11.3° with large uncertainties, up to 40%, because these events are associated to large local packing fluctuations which induces weak surface activities defined by an arbitrary threshold of $S/S_0=0.5$ (see Section II C). The dependency between θ_p and h is thus not obvious. The interprecursor angle $\Delta\theta$, defined as an average parameter over N_p observations, is more representative of the dynamic of the bead destabilization: it ranges between 0.9 and 1.4° and as a first approximation, it linearly increases with the packing height. By linked correlation, the number N_p of detected events decreases with h .

For scraped surface experiments, we have drawn the same linear slopes for the evolution of mean $\Delta\theta$ and N_p

only when $n_l > 40$ (see section III A) and they are associated to low error bars. Only the initial values are different 0.89° for $\Delta\theta$ and 16.1 for N_p . In the same manner, measurements of θ_p are larger and constant, about 13.5° , and also more reproducible than for soft leveled surfaces: scraping the surface tends to compact the superficial bead layer, for which effects are an increase of the stability angle and stronger events associated to larger activities, *i.e.* events for $S/S_0 > 0.5$ can be detected with more confidence. According to Eq. 1, this suggests a maximum stability angle of scraped surface packings about 25.5° when $n_l > 40$, in good agreement with the results presented above.

When $n_l < 40$, θ_p increases up to 16° when precursory events appear.

IV. INFLUENCE OF THE INCLINATION SPEED

In this section, we study the influence of the packing inclination speed, in the range $1.7\text{--}15^\circ/\text{min}$, on the avalanche and precursory events. For each experimental speed conditions, we have also reproduced between 8 and 15 similar experiments to highlight representative results. The choices of the different heights and surface couplings for the detailed analysis was induced by the observation of θ_A in Fig 2:

- when h is small (for example, $h = 4\text{ cm}$) and up to the discontinuity, the maximum stability angles are similar for the two surface fabrications
- when h is large (up to maximal $h = 18.5\text{ cm}$), the two maximum stability angles are also similar
- between these two limits, the difference is crucial just after the discontinuity ($H = 7.8\text{ cm}$) which suggest to analyze the two surface cases in this range: close to $h = 10\text{ cm}$.

So, in conclusion, soft leveled surface experiments have been performed with packing heights $h = 4$ and 10 cm and scraped surface experiments with $h = 10$ and 18.5 cm ;

A. Behavior of the maximum stability angle

As previously, for each experiment, we measure the maximum stability angle θ_A of the bead packing. The results are plotted in Fig. 4 which also shows the error bars of the measurements for both soft leveled (with $h = 4$ and 10 cm) and scraped surfaces (with $h = 10$ and 18.5 cm).

Soft leveled surface experiments are characterized by a continuous non linear increase of the maximum stability angle θ_A with the inclination speed: it increases from 22.2 to 23.5° for a packing height of $h = 4\text{ cm}$ and the

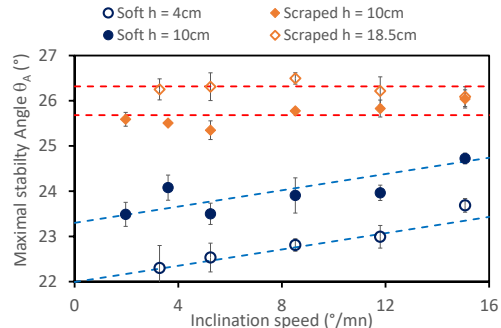


FIG. 4. Maximal stability angle θ_A measured as a function of the inclination speed with soft leveled (disks) or scraped (diamonds) surfaces and different packing heights. The dashed lines for the scraped surfaces are drawn horizontally and, for the soft leveled surface, they are just drawn for eyes guide without theoretical explanations. Error bars are associated to 8-15 similar experiments.

behavior is similar for $h = 10\text{ cm}$ where θ_A increases from 23.4 to 24.5° . The small increase is linked to the increase of the numbers of layers which implies higher internal stability. Indeed, the effect of h observed here is in agreement with the previous analyzes dedicated to the effects induced by the packing height (Fig. 2). In these soft leveled cases, the contact stiffness is weak and the superficial beads are more sensitive to inertia effects, which increase with the inclination speed, in agreement with previous experiments [35–37].

For the the scraped surface experiments, as we are at a height h which is higher than the discontinuity value ($h = 7.8\text{ cm}$) for θ_A , we can observe also here a nearly constant maximum stability angles θ_A , about 25.7 and 26.5° for packing heights $h = 10$ and 18.5 cm , respectively. The difference of 0.8° can fall into the uncertainty of the measurements performed for the previous analyzes (Fig. 2), already pointed out.

B. Behavior of the precursory events

As previously described (section III B), for each experiment (soft leveled or scraped surfaces), we also measure the characteristic parameters θ_p , $\Delta\theta$ and N_p associated to the precursory events and we have plotted their average in Fig. 5.

When the inclination speed increases, the uncertainties of the first precursor appearance increase naturally due to two additional effects coupled with the inertial effect: less accuracy for the image detection (still only one image per second for the acquisition) and higher inherent vibrations of the full setup linear actuator.

For all the four cases studied here, the first precursor appearance angles θ_p increase with the inclination speed

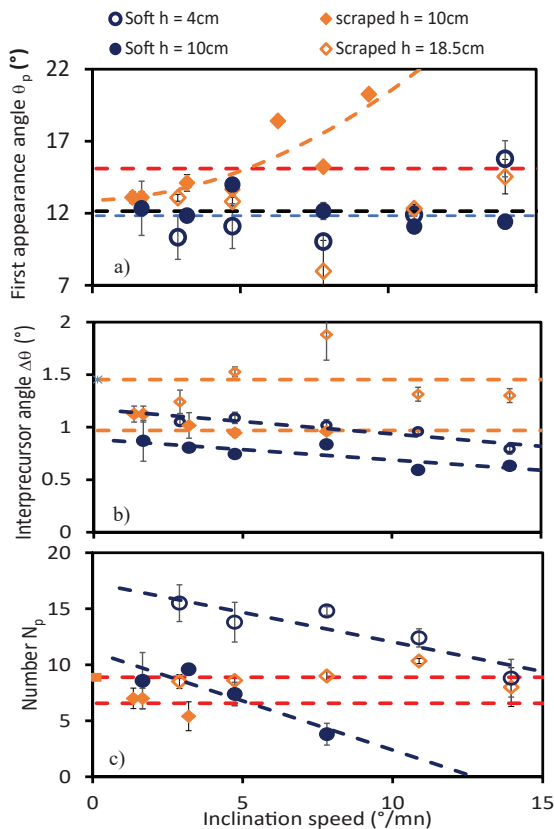


FIG. 5. Characteristic parameters of the precursory events measured as a function of the inclination speed with soft leveled (disks) or scraped (diamonds) surfaces and different packing heights. (a) represents the average of first precursor event θ_p . (b) and (c) are coupled to represent the behavior between $\Delta\theta(i)$ and $N_p(i)$.

and depend on the surface preparation: for the soft leveled surface (circle), the value starts around $\sim 10.5^\circ$ and ends around $\sim 13.5^\circ$, for the scraped surface (diamond), they start close to $\sim 13^\circ$ and ends at $\sim 20^\circ$. Naturally, it is less and less evident to generate and, by consequence, detect precursors when the inclination speed is high. In Fig. 5(a), we can notice also that, for the full height of the scraped surface ($h = 18.5 \text{ cm}$), the first precursor appearance can be observed as constant in the full range of speeds. This assumption is in accordance with the previous observation of the non-dependence of the maximal stability angle θ_A .

Fig. 5(b-c) shows the same combined information about the mean angle between successive precursors $\Delta\theta$ and N_p their mean number versus the inclination speed. As previously noticed, we can observe globally that, for the scraped surface, these two parameters are constant and for the soft leveled surface, they vary due to less and less internal superficial stress for smaller height h or higher speed.

Indeed, with a soft leveled surface, the packing is characterized by both an inter-precursor angle and a number

of inter-precursors that decrease linearly with the inclination speed. The inter-precursor angles $\Delta\theta$ vary from 1° to about 0.7° for $h = 4 \text{ cm}$ and from 0.9 to about 0.6° for $h = 10 \text{ cm}$. The numbers of inter-precursors N_p vary, in the same time, from 15 to 10 for $h = 4 \text{ cm}$ and from 10 to 0 for $h = 10 \text{ cm}$. We have to mention that, for the inclination angle θ higher than 18° , some superficial continuous slidings of superficial grains can appear without producing an avalanche which make the optical detection of precursors impossible in these cases. Of course, this problem avoids the use of these data for the averaging.

With a scraped surface, the packing is characterized by a constant inter-precursor angle $\Delta\theta$ about 1.5° for $h = 18.5 \text{ cm}$ and about 1° for $h = 10 \text{ cm}$. N_p is about 9 precursors for $h = 18.5 \text{ cm}$ and about 7 for $h = 10 \text{ cm}$. These results confirm also the observation made previously for the other scraped surface results: no evolution of parameters with either the height or the inclination speed for values of height higher than the transition limit of $h = 7.8 \text{ cm}$ (see section III A).

V. DISCUSSION AND CONCLUSION

The analysis of around 10 to 15 'identical' experiments (*i.e.* same history of fabrication and physical and mechanical parameters) have allowed us to use them with enough good reproducible results to deduce some conclusions about these different experimental protocols.

By opposition of the classical well-known results of the maximal stability angle θ_A and precursors appearances [4–7, 18], we have demonstrated that the packing preparation history (*i.e.* soft leveled or scraped surface) is, somehow, more crucial than the packing height minimal critical limit, which defines the available range of possible observations, classically presented in the previous studies of avalanches and precursor events for tilted granular packings. Otherwise, the soft leveled surface cases are, always, producing more evolving results than the scraped ones. So, in a practical point of view, the use of scraped surface implies that the experiments can be performed at a 'high inclination' speed, allowing performing a larger number of experiments for studies requiring statistical approaches and producing also less uncertainties results.

Main results and conclusions are defining the good use for our future works made in our laboratory for studying more complex behaviors such as playing with different lengths and widths of the box, inclination speed, oscillation cycles $\pm\theta_c$, environmental conditions (humidity range RH) or adding other detection techniques such as mechanical or acoustical sensors.

ACKNOWLEDGMENTS

We would like to thanks P. Chasle for all the developments of our complex LabVIEW™ code and Y. Robert

and G. Pecheul for the mechanical realizations.

-
- [1] A. J. Liu and S. R. Nagel, Annual Reviews of Cond. Mat. Phys. **1**, 347 (2010).
- [2] L. Oger, A. Vidales, R. Uñac, and I. Ippolito, Granular Matter **15**, 629 (2013).
- [3] Y. Zhang and C. S. Campbell, J. Fluid Mech. **237**, 541 (1992).
- [4] M. A. Aguirre, N. Nerone, I. Ippolito, A. Calvo, and D. Bideau, Granular Matter **3**, 75 (2001).
- [5] N. Nerone, M. Aguirre, A. Calvo, D. Bideau, and I. Ippolito, Phys. Rev. E **67**, 011302 (2003).
- [6] S. Kiesgen de Richter, G. Le Caër, and R. Delannay, Journal of Statistical Mechanics: Theory and Experiment **04**, P04013 (2012).
- [7] M. Duranteau, *Dynamique granulaire à l'approche de l'état critique*, Ph.D. thesis, Université Rennes 1 (2013).
- [8] V. Y. Zaitsev, P. Richard, R. Delannay, V. Tournat, and V. E. Gusev, EPL (Europhysics Letters) **83**, 64003 (2008).
- [9] M. Duranteau, V. Tournat, V. Zaitsev, R. Delannay, and P. Richard, in *Powders and Grains 2013*, Vol. 1542 (AIP, 2013) pp. 650–653.
- [10] S. Kiesgen de Richter, *Etude de l'organisation des réarrangements d'un milieu granulaire sous sollicitations mécaniques*, Ph.D. thesis, Université de Rennes1 (2009).
- [11] S. Kiesgen de Richter, V. Y. Zaitsev, P. Richard, R. Delannay, G. Le Caër, and V. Tournat, Journal of Statistical Mechanics: Theory and Experiment **11**, P11023 (2010).
- [12] R. Delannay, M. Duranteau, and V. Tournat, Comptes Rendus Physique **16**, 45 (2015).
- [13] P. Boltenhagen, The European Physical Journal B **12**, 75 (1999).
- [14] S. Courrech du Pont, P. Gondret, B. Perrin, and M. Rabaud, Europhysics Letters (EPL) **61**, 492 (2003).
- [15] W. Bi, R. Delannay, P. Richard, N. Taberlet, and A. Valance, Journal of Physics: Condensed Matter **17**, S2457 (2005).
- [16] J. Métayer, *Stabilité et propriétés rhéologiques d'empilements granulaires confinés.*, Ph.D. thesis, Université de Rennes I (2008).
- [17] P. Evesque, D. Fargeix, P. Habib, M. P. Luong, and P. Porion, Journal de Physique I **2**, 1271 (1992).
- [18] M. A. Aguirre, N. Nerone, A. Calvo, I. Ippolito, and D. Bideau, Physical Review E **62**, 738 (2000).
- [19] N. Gravish and D. I. Goldman, Physical Review E **90**, 032202 (2014).
- [20] A. Kabla, G. Debrégeas, J.-M. di Meglio, and T. J. Senden, Europhysics Letters (EPL) **71**, 932 (2005).
- [21] A. Jarray, V. Magnanimo, and S. Luding, Powder Technology **341**, 126 (2019).
- [22] D. Mehta and M. C. Hawley, Industrial & Engineering Chemistry Process Design and Development **8**, 280 (1969).
- [23] L. Oger, J. P. Troadec, D. Bideau, J. A. Dodds, and M. J. Powell, Powder Technol. **46**, 121 (1986).
- [24] Y. Bertho, F. Giorgiutti-Dauphiné, and J.-P. Hulin, Physical Review Letters **90**, 144301 (2003).
- [25] W. Dai, J. Reimann, D. Hanaor, C. Ferrero, and Y. Gan, Granular Matter **21**, 26 (2019).
- [26] J. Lin, H. Chen, R. Zhang, and L. Liu, Materials Characterization **154**, 335 (2019).
- [27] L. Oger, R. Delannay, and Y. Le Gonidec, in *Powders and Grains 2021*, Vol. 249, edited by M. Aguirre, S. Luding, L. Pugnaloni, and R. Soto (EDP Sciences, 2021) p. 03023.
- [28] L. Oger, C. El Tannoury, R. Delannay, Y. Le Gonidec, I. Ippolito, Y. L. Roht, and I. Gómez-Arriaran, Physical Review E **101**, 022902 (2020).
- [29] D. Bideau, E. Guyon, and L. Oger, in *Disorder and Fracture*, Vol. 204, edited by J. C. Charmet, S. Roux, and E. Guyon (Springer US, Boston, MA, 1990) NATO ASI series (series b: physics) ed., pp. 255–268.
- [30] N. Nerone, M. Aguirre, A. Calvo, I. Ippolito, and D. Bideau, Physica A **283**, 218 (2000).
- [31] C. Schneider, W. Rasband, and K. Eliceiri, Nature Methods **9**, 671 (2012).
- [32] E. Guyon and J. P. Troadec, *Le sac de billes* (Ed. Odile Jacob, 1994).
- [33] S. J. Antony, Philos. Trans. R. Soc. A: Math. Phys. Eng. Sci. **365**, 2879.
- [34] M. A. Aguirre, N. Nerone, A. Calvo, I. Ippolito, and D. Bideau, *Traffic and Granular Flow* (Springer, Berlin, Heidelberg, Berlin New York, 2000) pp. 489–494.
- [35] G. H. Ristow, Europhys. Lett. **34**, 263 (1996).
- [36] A. Jarray, V. Magnanimo, M. Ramaioli, and S. Luding, *Powders and Grains*, EPJ Web of Conferences **140**, 03078 (2017).
- [37] T. Pöschel and V. Buchholtz, Chaos, Solitons, and Fractals **5**, 1901 (1995).